Inorg. Chem. **2004**, *43*, 7151–7161

Effects of Peripheral Substituents and Axial Ligands on the Electronic Structure and Properties of Iron Phthalocyanine

Meng-Sheng Liao,[†] Tapas Kar,[†] Sergiu M. Gorun,[‡] and Steve Scheiner*[,†]

Department of Chemistry & Biochemistry, Utah State University, Logan, Utah 84322-0300, and Department of Chemistry & Environmental Science, New Jersey Institute of Technology, Newark, New Jersey 07102

Received October 31, 2003

The effects of peripheral substituents and axial ligands on the electronic structure and properties of iron phthalocyanine, H_{16}PcFe, have been investigated using a DFT method. Substitution by electron-withdrawing fluorinated groups alters the ground state of H_{16}PcFe and gives rise to large changes in the ionization potentials and electron affinity. For the six-coordinate adducts with acetone, H_2O, and pyridine, the axial coordination of two weak-field ligands leads to an intermediate-spin ground state, while the strong-field ligands make the system diamagnetic. The electronic configuration of a ligated iron phthalocyanine is determined mainly by the axial ligand-field strength but can also be affected by peripheral substituents. Axial ligands also exert an effect on ionization potentials and electron affinity and can, as observed experimentally, even change the site of oxidation/reduction.

1. Introduction

Metal phthalocyanines (PcMs) have attracted considerable interest because of their numerous applications in industry,[1] which benefit from the ease of tuning or modifying the properties of the ring system. One of the principal strategies for the molecular design and control of properties of PcMs involves ring substitution, and so far many novel substituted phthalocyanines have been synthesized. Compared to pure PcMs, some of the metal complexes with multiple electron-withdrawing peripheral substituents are more stable and more active catalysts for a variety of hydrocarbon oxygenation reactions.[1b,i,k] The high stability of the substituted metal complexes may be attributed to the electron-withdrawing substituents at the periphery of the macrocycle that cause a large increase in the ionization potential (IP) of the system, and thus protect the catalyst from oxidative destruction. Recently, several novel octakis(perfluoro *i*-C_3F_7)(perfluoro)-PcM compounds have been synthesized.[2] F_{64}PcM (M = Zn,[2a] Co,[2b] Fe,[2c]) complexes can be used to produce singlet oxygen,[2a] catalyze the aerobic formation of R′—HC═PR_3 ylides (R′ = acetyl, R = alkyl, aryl) via oxidation,[2b] and oxygenate C—H bonds.[2c] These F_{64}PcM species are stable under harsh oxygenation conditions. In contrast, it was found that even fluorinated PcFe's and related porphyrin complexes have limited stability as catalysts for oxidation reactions.[3]

To obtain insight into the changes induced by peripheral substitution, theoretical calculations have been carried out

* To whom correspondence should be addressed. E-mail: scheiner@cc.usu.edu.
[†] Utah State University.
[‡] New Jersey Institute of Technology.

(1) (a) Chambrier, I.; Cook, M. J.; Wood, P. T. *Chem. Commun.* **2000**, 2133. (b) Moser, F. H.; Thomas, A. L. *The Phthalocyanines*; CRC Press: Boca Raton, FL, 1983. (c) Berezin, B. D. *Coordination Compounds of Porphyrins and Phthalocyanines*; J. Wiley and Sons: New York, 1981. (d) Borsenger, P. M.; Weiss, D. S. *Organic Photoreceptors for Imaging System*; Marcel Dekker: New York, 1993. (e) Locklin, J.; Shinbo, K.; Onishi, K.; Kaneko, F.; Bao, Z. N.; Advincula, R. C. *Chem. Mater.* **2003**, *15*, 1404. (f) Bao, Z. N.; Lovinger, A. J.; Dodabalapur, A. *Adv. Mater.* **1997**, *9*, 42. (g) Kuder, J. E. *J. Imaging Sci.* **1988**, *32*, 51. (h) Sadaoka, Y.; Jones, T. A.; Göpel, W. *Sens. Actuators, B* **1990**, *I*, 148. (i) Mckeown, N. B. *Phthalocyanine Materials*, Cambridge University Press: Cambridge, 1998. (j) Orti, E.; Bredas, J.-L. *J. Am. Chem. Soc.* **1992**, *114*, 8669. (k) *Phthalocyanines: Properties and Applications*; Leznoff, C. C., Lever, A. B. P., Eds.; VCH Publishers: New York, 1989, 1993, 1996; Vols. 1−4.

(2) (a) Bench, B. A.; Beveridge, A.; Sharman, W. M.; Diebold, G. J.; van Lier, J. E.; Gorun, S. M. *Angew. Chem., Int. Ed.* **2002**, *41*, 748. (b) Bench, B. A.; Brennessel, W. W.; Lee, H.-J.; Gorun, S. M. *Angew. Chem., Int. Ed.* **2002**, *41*, 750. (c) Lee, H.-J.; Brennessel, W. W.; Brucker, W. J.; Lessing, J. A.; Young, V. G., Jr.; Gorun, S. M. To be submitted.

(3) (a) Sorokin, A. B.; Tuel, A. *Catal. Today* **2000**, *57*, 45. (b) Moore, K. T.; Horvath, I. T.; Therien, M. J. *Inorg. Chem.* **2000**, *39*, 3125. (c) Kadish, K. M.; Van Caemelbecke, E.; D'Souza, F.; Lin, M.; Nurco, D. J.; Medforth, C. J.; Forsyth, T. P.; Krattinger, B.; Smith, K. M.; Fukuzumi, S.; Nakanishi, I.; Shelnutt, J. A. *Inorg. Chem.* **1999**, *38*, 2188. See also: Showalter, M. C.; Nenoff, T. M.; Shelnutt, J. A. *SAND96-2577*. (d) Wijesekera, T. P.; Lyons, J. E.; Ellis, P. E., Jr. *Catal. Lett.* **1995**, *36*, 69. (e) Lyons, J. E.; Ellis, P. E., Jr. *Catal. Lett.* **1991**, *8*, 45. (f) Nappa, M. J.; Tolman, C. A. *Inorg. Chem.* **1985**, *24*, 4711.

10.1021/ic035263j CCC: $27.50
Published on Web 09/28/2004

here for R_fPcFe with multiple R_f perfluoroalkyl groups, as well as for the parent perfluorinated F_{16}PcFe. The latter system was reported by Jones and Twigg 35 years ago.[4] PcFe was chosen as a prototype here also because this system is interesting in its own right. The d^6 Fe^{II} ion can exhibit three spin states: $S = 0$ (low spin), $S = 1$ (intermediate spin), and $S = 2$ (high spin). Experimental investigations[5−7] have definitively established the $S = 1$ ground state for the planar, tetracoordinate H_{16}PcFe but differ in their conclusions regarding the details of the ground-state electronic configuration. A $^3B_{2g}$ ground state was originally suggested for H_{16}PcFe on the basis of magnetic work,[6] but later magnetic circular dichroism spectra have shown that the ground state is in fact $^3A_{2g}$.[7] Our own previous calculation[8] supported the experimental assignment of H_{16}PcFe as $^3A_{2g}$. The present study is intended to examine the influence of strongly electron-withdrawing substituents on the electronic structure and properties of PcFe complexes.

X-ray crystal structural data have been reported for the six-coordinate adducts of F_{64}PcFe with H_2O and with pyridine (Py).[2c] Both F_{64}PcFe$(H_2O)_2$ and F_{64}PcFe$(Py)_2$ are diamagnetic ($S = 0$), in contrast to axially coordinated, perfluorinated F_{16}PcFe$(Ace)_2$ (where Ace stands for acetone). The latter system exhibits an intermediate-spin state ($S = 1$) with measured effective magnetic moment of 3.3 ± 0.2 μ_B.[4] On the other hand, F_{16}PcFe in pyridine solution produces a diamagnetic bis-pyridine adduct F_{16}PcFe$(Py)_2$,[4] similar to F_{64}PcFe$(Py)_2$. The capacity for additional coordination of axial ligands is one of the most important properties of the PcFe molecules. A second purpose of this work is an examination of the sensitivity of electronic structure and properties of the ligated iron phthalocyanines to the nature of the axial ligands.

The large size and complexity of the molecules makes it difficult to use standard ab initio methods. Fortunately, the refinement of density-functional theory (DFT) methods in recent years has made them a suitable, and sometimes preferable, alternative to ab initio approaches. While the DFT method, based on the Kohn−Sham one-electron equation, is not generally applicable to excited states, it can be used to good effect to calculate the lowest-energy state of each symmetry for a particular system.[9] There have been many applications of DFT methods to calculations of excited states in unligated and ligated iron porphyrins (e.g., ref 10a−e). To assess the validity of the ADF method used in this work (see section 2), calculations on iron porphine (PFe) have also been carried out here (see also ref 11), and a comparison of the results among different computational methods is reported in Appendix 1. The success of ADF calculations on iron porphyrins[10d,e,11] lends confidence in applying the same program to the iron phthalocyanines.

2. Computational Details

The molecular structure of the parent iron phthalocyanine H_{16}PcFe is illustrated in Figure 1a, and that of (perfluoro *i*-C_3F_7)−(perfluoro) phthalocyanine, F_{64}PcFe, is in Figure 1e. In order to examine in detail the effect of electron-withdrawing substituents, the perfluoro *i*-C_3F_7 and perfluoro groups were added in stages. First, all benzo H atoms of H_{16}PcFe were replaced by F, to give F_{16}PcFe, Figure 1b. Next, the two peripheral F atoms on each benzo group were replaced by CF_3, yielding the F_{32}PcFe species of Figure 1c. F_{48}PcFe refers to the species illustrated in Figure 1d, wherein the latter CF_3 groups were enlarged to CF_2CF_3. The final goal, F_{64}PcFe in Figure 1e, corresponds to the replacement of a F atom of each CF_2 portion of the CF_2CF_3 groups by CF_3, yielding $CF(CF_3)_2$ groups. It should be noted that the *i*-C_3F_7 (in F_{64}PcFe), C_2F_5 (in F_{48}PcFe), and CF_3 (in F_{32}PcFe) groups all have a C atom bound to the aromatic ring, and thus, the terminal CF_3 group, which is modeled by F, is separated from the Pc ring by this C. The F_{16}PcFe system (Figure 1b) is fundamentally different, in that each of the eight *i*-C_3F_7 groups in F_{64}PcFe is replaced by a single F atom, and so each aromatic benzo ring in F_{16}PcFe has four F atoms bonded directly to it. An important consequence is the possibility of F π-back-bonding in the latter complex, but not in the former, R_fPcFe, ones.[2]

All calculations were carried out using the Amsterdam Density Functional (ADF) program package (version 2.0.1) developed by Baerends and co-workers.[12] A triple-ζ STO basis was used for Fe 3s−4s shells plus one 4p polarization function, a triple-ζ basis for C/N/O 2s−2p shells plus one 3d polarization function, a double-ζ basis for F 2s−2p shells, and a double-ζ basis for the H 1s shell. It has been shown that high-quality basis sets (triple-ζ basis plus one polarization function) are required for the atoms within the macrocycle ring of the phthalocyanine in order to obtain the correct ground states of H_{16}PcFe and its derivatives.[13] The inner orbitals, i.e., 1s−2p for Fe and 1s for C/N/O/F, were considered as core and kept frozen according to the frozen-core approximation.[12a] Among the various exchange-correlation potentials available, the density-parametrization form of Vosko, Wilk, and Nusair (VWN)[14] plus Becke's gradient correction for exchange (B)[15] and Perdew's gradient correction for correlation (P)[16] were employed. It has been shown that the combined VWN-B-P functional can provide accurate bonding energies for both main-group[17] and transition metal[18] systems. The effect of different density-functional formalisms has also been examined (see Appendix 2). (No hybrid density functionals that mix nonlocal exchange with exact Hartree−Fock exchange are available in the present ADF program.) Relativistic corrections of the valence electrons were calculated by the quasirelativistic (QR) method.[19] For the open-shell states, the

(4) Jones, J. G.; Twigg, M. V. *Inorg. Chem.* **1969**, *8*, 2018.
(5) Dale, B. W.; Williams, R. J. P. *J. Chem. Phys.* **1968**, *49*, 3445.
(6) Barraclough, C. G.; Martin, R. L.; Mitra, S. *J. Chem. Phys.* **1970**, *53*, 1643.
(7) Stillman, M. J.; Thomson, A. J. *J. Chem. Soc., Faraday Trans. 2* **1974**, *70*, 790.
(8) Liao, M.-S.; Scheiner, S. *J. Chem. Phys.* **2001**, *114*, 9780.
(9) (a) Ziegler, T.; Rauk, A.; Baerends, E. J. *Theor. Chim. Acta* **1977**, *43*, 261. (b) Jones, R. O.; Gunnarson, O. *Rev. Mod. Phys.* **1989**, *61*, 689.
(10) (a) Delley, B. *Physica B* **1991**, *172*, 185. (b) Matsuzawa, N.; Ata, M.; Dixon, D. A. *J. Phys. Chem.* **1995**, *99*, 7698. (c) Rovira, C.; Kunc, K.; Hutter, J.; Ballone, P.; Parrinello, M. *J. Phys. Chem. A* **1997**, *101*, 8914. (d) Kozlowski, P. M.; Spiro, T. G.; Bérces, A.; Zgierski, Z. *J. Phys. Chem. B* **1998**, *102*, 2603. (e) Kozlowski, P. M.; Spiro, T. G.; Zgierski, M. Z. *J. Phys. Chem. B* **2000**, *104*, 10659.
(11) Liao, M.-S.; Scheiner, S. *J. Chem. Phys.* **2002**, *117*, 205.
(12) (a) Baerends, E. J.; Ellis, D. E.; Roos, P. *Chem. Phys.* **1973**, *2*, 41. (b) te Velde, G.; Baerends, E. J. *J. Comput. Phys.* **1992**, *99*, 84.
(13) Liao, M.-S.; Scheiner, S. Unpublished results.
(14) Vosko, S. H.; Wilk, L.; Nusair, M. *Can. J. Phys.* **1980**, *58*, 1200.
(15) Becke, A. D. *Phys. Rev. A* **1988**, *38*, 3098.
(16) Perdew, J. P. *Phys. Rev. B* **1986**, *33*, 8822.
(17) Johnson, B. G.; Gill, P. M. W.; Pople, J. A. *J. Chem. Phys.* **1993**, *98*, 5612.
(18) Li, J.; Schreckenbach, G.; Ziegler, T. *J. Am. Chem. Soc.* **1995**, *117*, 486.

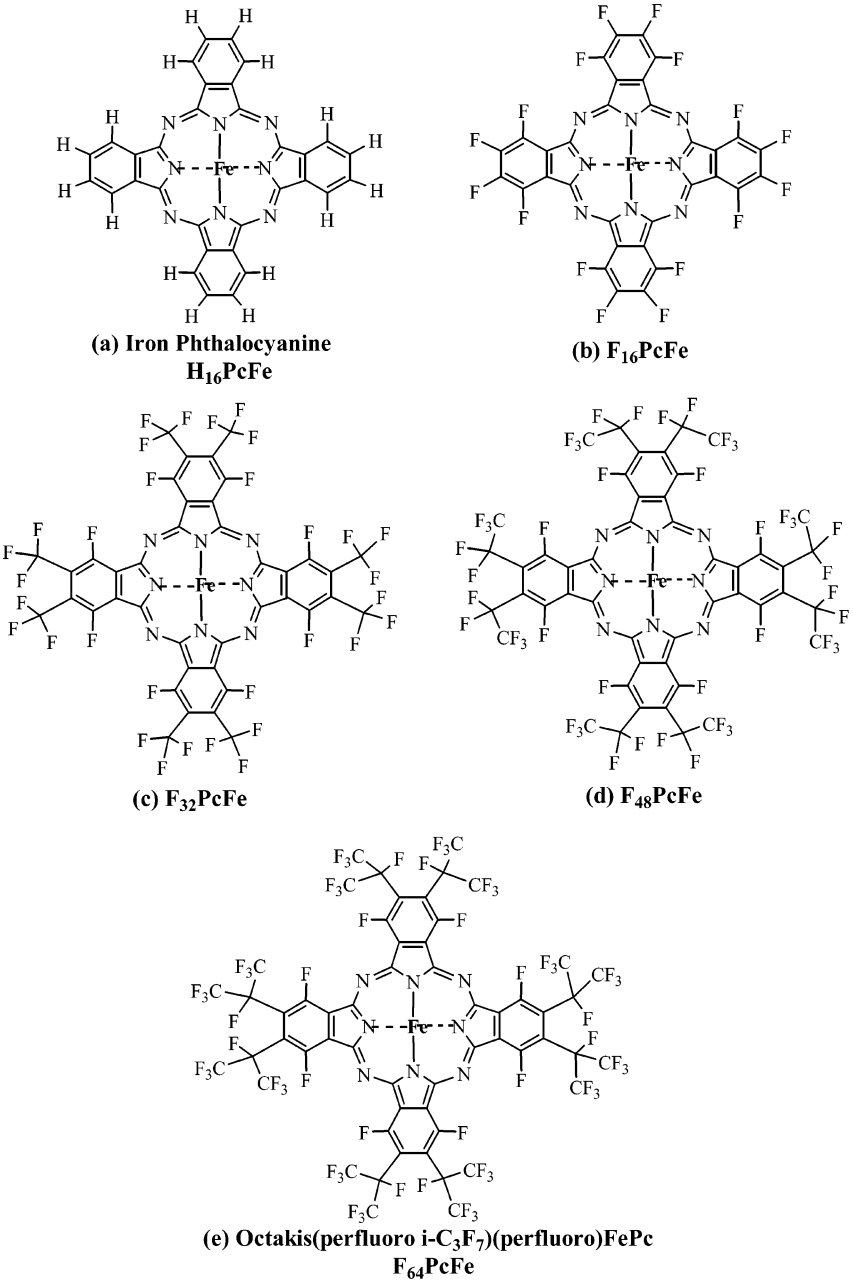

Figure 1. Molecular structures of iron phthalocyanine (H_{16}PcFe) and its fluorosubstituted derivatives.

unrestricted Kohn−Sham (UKS) spin-density functional approach was adopted. The UKS equation is the analogue of the unrestricted Hartree−Fock (UHF) equation; the N-particle wave function is a single determinant and not necessarily an eigenfunction of the spin operator $\hat{S}^2$. There is no implementation of an evaluation of $|\hat{S}^2|$ in the present ADF program, and hence, spin contamination could not be directly assessed. In this case, we performed a set of additional spin-restricted (R) calculations for several complexes, the purpose of which is to examine whether the UKS and RKS calculated geometric parameters are similar.

Our analysis focuses on the following properties of the systems considered: electronic structure configurations, charge distributions on the metal, Fe−Pc binding energies, critical geometric parameters, ionization potentials, and electron affinities. We have not calculated electron excitation energies (E^{exc}'s) that are related to electronic ultraviolet (UV)−visible (vis) absorption spectra. In the present ADF program, E^{exc} can be evaluated using the time-dependent density-functional theory (TDDFT) method. However, the implementation of this method supports only closed-shell molecules. Most of the systems studied here (including all unligated PcFes) have an open-shell state, and we are hence unable to directly calculate the effects of peripheral substituents and axial ligands upon E^{exc}.

It should be understood that the calculations deal specifically with free molecules, i.e., gas phase, while the experimental results relate to the solid state or solution.

3. Results and Discussion

3.1. H_{16}PcFe, F_{16}PcFe, F_{32}PcFe, and F_{48}PcFe. For computational purposes, the symmetry and geometry of the first metal coordination sphere as well as that of the entire Pc molecule is of critical importance. Unsubstituted transition metal PcM's have been shown to have square planar D_{4h}

(19) Ziegler, T.; Tschinke, V.; Baerends, E. J.; Snijders, J. G.; Ravenek, W. *J. Phys. Chem.* **1989**, *93*, 3050.

Table 1. Calculated Relative Energies (E's, eV) for Different Configurations in $H_{16}PcFe$, $F_{16}PcFe$, $F_{32}PcFe$, and $F_{48}PcFe$

configuration[a]					E (R)[b]			
b_{2g}/d_{xy}	a_{1g}/d_{z^2}	$1e_g/d_\pi$	$b_{1g}/d_{x^2-y^2}$	state	$H_{16}PcFe$	$F_{16}PcFe$	$F_{32}PcFe$	$F_{48}PcFe$
2	2	2	0	$^3A_{2g}$	0 (1.922)[b]	0 (1.922)	0 (1.925)	0 (1.924)
2	1	3	0	^3E_g (A)	0.05 (1.929)	0.01 (1.926)	−0.02 (1.930)	−0.02 (1.926)
1	1	4	0	$^3B_{2g}$	0.07 (1.927)	0.04 (1.923)	−0.05 (1.924)	−0.05 (1.922)
1	2	3	0	^3E_g (B)	0.53 (1.916)	0.53 (1.915)	0.47 (1.918)	0.47 (1.915)
1	2	2	1	$^5A_{1g}$	1.13 (1.982)	1.07 (1.981)	1.08 (1.984)	1.10 (1.978)
1	1	3	1	^5E_g	1.17 (1.987)	1.08 (1.985)	1.04 (1.988)	1.04 (1.985)
2	1	2	1	$^5B_{2g}$	1.50 (1.986)	1.42 (1.980)	1.39 (1.988)	1.43 (1.980)
2	0	4	0	$^1A_{1g}$	1.42 (1.941)	1.35 (1.938)	1.29 (1.942)	1.28 (1.938)

[a] Orbital energy levels illustrated in Figure 2. [b] Values in parentheses refer to optimized Fe−N(eq) bond length (in Å) for the pertinent state.

symmetry.[8] X-ray crystal structure data[2c] indicate that substituted $F_{64}PcFe$ possesses in the solid state a planar aromatic unit, as required by the D_{4h} symmetry. The solution UV−vis spectra are also consistent with D_{4h} symmetry, as departure from planarity for a nonperipherally substituted PcFe, which results in the lowering of molecular symmetry to D_{2d}, induces absorptions at wavelengths longer than those of the Q-bands.[20] Such absorptions are not observed in the spectra of $F_{64}PcFeL_2$, with L = H_2O or Py, recorded in various solvents.[2c] A search of the Cambridge Crystallographic Database (CCDB) for hexacoordinated Fe(II) phthalocyanines with R < 7% revealed nine complexes, all of $H_{16}PcFe$ type, i.e., with unsubstituted peripheral ligand (see Supporting Information). Their average Fe−N (phthalocyanine) bond length, $R_{Fe-N(eq)}$ = 1.935(6) Å (variance = 3.38×10^{-5}), a value which is statistically identical with the 1.938(2) Å value of the Fe−N(eq) bond lengths of $F_{64}PcFe(Py)_2$. Moreover, in all the literature complexes, the Fe is located in the plane of the N4 equatorial coordinating set, a feature preserved in $F_{64}PcFe(Py)_2$ and $F_{64}PcFe(H_2O)_2$,[2c] as well as the Zn and Co complexes of the $F_{64}Pc$ ligand.[2a,b] The invariability of the FeN_4 chromophore geometry upon substitution of the peripheral H positions by i-C_3F_7 R_f groups strongly suggests that the geometry will not change for steric reasons when the i-C_3F_7 groups are replaced by less bulky groups in $F_{16}PcFe$, $F_{32}PcFe$, and $F_{48}PcFe$. The same conclusion can be drawn for the nonperipheral substitution of H, Figure 1a, by F in all R_fPcFe complexes, including the most sterically hindered, but planar, ones, $F_{64}PcFe(L)_2$.

Therefore, $F_{16}PcFe$, $F_{32}PcFe$, and $F_{48}PcFe$ were all assumed to belong to the D_{4h} point group. If some limited distortion from planarity of the macrocycle core does occur, this was shown to have only a very small influence on the calculated molecular properties.[11,21] After placement of the molecule in the xy plane, the five Fe 3d-orbitals transform as a_{1g} (d_{z^2}), b_{1g} ($d_{x^2-y^2}$), e_g (d_π, i.e., d_{xz} and d_{yz}), and b_{2g} (d_{xy}). Different occupancies of six electrons in these d-orbitals can yield a number of possible low-lying electronic states. The purpose of this paper is to elucidate the ground state and several low-lying excited states that are usually considered in the literature. Geometry optimization was performed for all states of each molecule. The program allows one to assign electrons to specific molecular orbitals (MOs), and therefore, every state can be obtained by explicit occupations of the necessary MOs. The procedure of geometry optimization is the same for each state. The energetic orderings of the various states are displayed in Table 1, along with the optimized Fe−N bond length of each.

We consider the unsubstituted $H_{16}PcFe$ first: the lowest energy electronic configuration is calculated to be $[...](b_{2g})^2(a_{1g})^2(1e_g)^2$, a $^3A_{2g}$ state, in agreement with the magnetic circular dichroism measurement.[7] The second lowest state, only 0.05 eV higher than $^3A_{2g}$, is ^3E_g wherein one of the a_{1g} electrons has been transferred to $1e_g$. The energy of $^3B_{2g}$ also comes quite close to that of $^3A_{2g}$. The lowest quintet is $^5A_{1g}$, lying 1.13 eV above the ground state. The closed-shell $^1A_{1g}$ configuration $(b_{2g})^2(a_{1g})^0(1e_g)^4$ lies higher than the ground state by 1.42 eV. As indicated in Table 1, the calculated Fe−N bond length for the S = 0 state, 1.94 Å, is slightly longer than the 1.92−1.93 Å range that characterizes the triplets. For the high-spin (S = 2) states, an occupied b_{1g} ($d_{x^2-y^2}$) orbital and its repulsive (antibonding) interaction with N lone pairs lead to lengthening of the Fe−N bond length to 1.98−1.99 Å. Two other density functionals were tested in the calculations and the results reported in the Appendix 2; they indicate that the nonlocal gradient corrections (to the local density functionals) play an important role in the calculations of the relative energies.

From $H_{16}PcFe$ to $F_{16}PcFe$, the ^3E_g−$^3A_{2g}$ energy gap essentially disappears entirely; the ^3E_g state of $F_{16}PcFe$ lies only 0.01 eV above $^3A_{2g}$, leaving the identity of the ground state in doubt. The $^3B_{2g}$−$^3A_{2g}$ energy gap is also reduced in $F_{16}PcFe$. On balance, the substitution of all 16 peripheral H-atoms with F-atoms barely changes the overall energetics of the various states or the Fe−N distances.

(20) Fukuda, T.; Homma, S.; Kobayashi, N. *Chem. Commun.* **2003**, 1574.

(21) Some controversies exist in the literature concerning the effects of nonplanar deformation on the optical spectra of porphyrins. Large red shifts in the UV−vis absorption bands are observed for highly encumbered porphyrins which were originally ascribed to nonplanar distortion. However, recent calculations by DiMagno et al. (*J. Am. Chem. Soc.* **1995**, *117*, 8279), and later by Ryeng and Ghosh (*J. Am. Chem. Soc.* **2002**, *124*, 8099), indicated that ruffling of porphyrins does not cause sizable red shifts in the electronic spectra of some free-base porphyrins. These authors argued that "the observed red shifts are not intrinsic to ring distortion, but result from different substituent effects in planar and nonplanar conformations." On the other hand, more recently, Haddad et al. (*J. Am. Chem. Soc.* **2003**, *125*, 1253) used a semiempirical INDO/CI method to show that nonplanar distortions indeed cause the red shifts and that the lack of large red shifts in the model calculations of DiMagno et al. and of Ryeng and Ghosh resulted from unphysical porphyrin structures obtained by artificial constraints imposed on the structures used in the calculations. The semiempirical results of Haddad may need to be verified by more sophisticated computational methods. The molecular properties considered here are total energies, bond lengths, ionization potentials, and electron affinities, and they are indeed scarcely affected by limited nonplanar distortions (see ref 11 for more details).

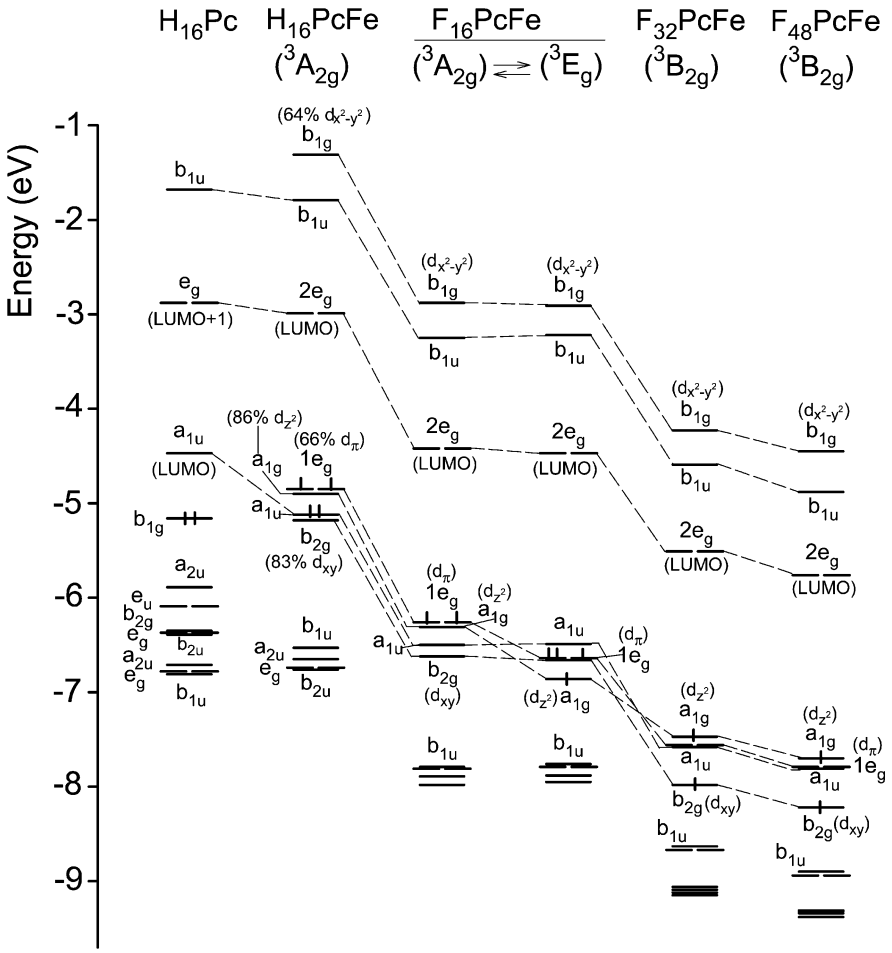

Figure 2. Orbital energy levels of $H_{16}Pc$ (on left, with no H atoms in the ring cage) and the various iron phthalocyanines.

The picture, however, changes considerably for $F_{32}PcFe$. The order of the three lowest states is $^3B_{2g} < {}^3E_g < {}^3A_{2g}$, opposite to the previous two cases. This substitution pattern also produces a uniform, albeit small, elongation of the Fe−N distances in the various states. On going from $F_{32}PcFe$ to $F_{48}PcFe$, the enhanced fluorosubstitution produces almost no change in any of the quantities reported in Table 1. This result implies that an F atom can very adequately mimic the effects of a CF_3 within a larger, aliphatic C_xF_y substituent, and so the simpler $F_{32}PcFe$ is able to reproduce the essential properties of the larger $F_{48}PcFe$ and by implication $F_{64}PcFe$.

More evidence for this contention comes from examination of Figure 2, which illustrates the valence molecular orbital (MO) energy levels for the ground states of the four molecules. For simplicity, and to avoid the complication of two sets of orbitals (α and β), the MO energy levels shown in the figure were obtained by spin-restricted calculations. In this case, for some open-shell systems such as $F_{32}PcFe$ and $F_{48}PcFe$, a singly occupied MO may lie lower than a doubly occupied MO. But this does not necessarily imply that an empty spin-orbital would lie lower than an occupied one.[22] To further clarify this point, Figure 3 displays the unrestricted MO energy levels for $F_{32}PcFe$, together with the restricted MOs for comparison. It may be clearly observed that all occupied spinors lie lower than the empty ones, in accordance with Janak's theorem.[23] (As usual, the restricted MO energies are all slightly shifted with respect to the unrestricted averages.)

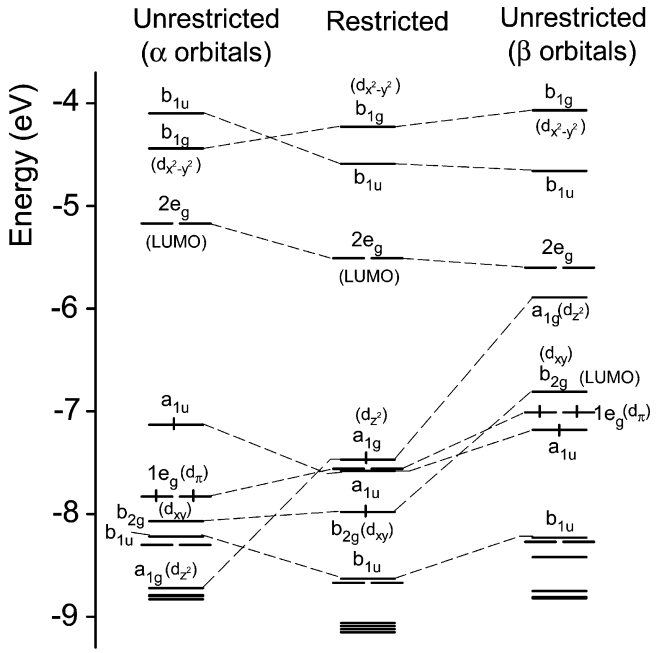

Figure 3. Unrestricted and restricted orbital energy levels of $F_{32}PcFe$.

We consider first $H_{16}PcFe$: the occupied MOs are divided into two groups. Those of higher energy are b_{2g}/d_{xy}, a_{1u}, a_{1g}/d_{z^2}, and $1e_g/d_\pi$, which are well separated from the lower-

Table 2. Comparison of the Fe−N(eq) Bond Lengths (in Å) Obtained by Spin-Restricted Kohn−Sham (RKS) and Spin-Unrestricted Kohn−Sham (UKS) Calculations

	H_{16}PcFE		F_{16}PcFe		F_{32}PcFe	
state	RKS	UKS	RKS	UKS	RKS	UKS
$^3A_{2g}$	1.911	1.922	1.910	1.922	1.915	1.925
^3E_g (A)	1.925	1.929	1.921	1.926	1.925	1.930
$^3B_{2g}$	1.921	1.927	1.918	1.923	1.920	1.924
^3E_g (B)	1.908	1.916	1.908	1.915	1.912	1.918
$^5A_{1g}$	1.976	1.982	1.975	1.981	1.978	1.984
^5E_g	1.980	1.987	1.979	1.985	1.981	1.988
$^5B_{2g}$	1.977	1.986	1.972	1.980	1.979	1.988

Table 3. Mulliken Orbital Populations and Atomic Charges (Q's) on Fe

	H_{16}PcFe	F_{16}PcFe	F_{32}PcFe	F_{48}PcFe
3d	6.59	6.58	6.59	6.59
4s	0.41	0.37	0.27	0.26
4p	0.26	0.25	0.27	0.26
Q_{Fe}	0.74	0.80	0.87	0.88

lying levels. The d_{z^2} and d_π orbitals, which are nearly degenerate, are weakly antibonding, higher in energy than the nonbonding d_{xy}, and represent a group of HOMOs. The a_{1u} orbital from the Pc ring lies between b_{2g} and a_{1g}. The $2e_g$ orbital represents the LUMO, which is mainly composed of the Pc antibonding π^* orbitals. The metal b_{1g} ($d_{x^2-y^2}$) is unoccupied and lies above the empty Pc b_{1u} orbital.

The F atoms are strongly electron-withdrawing, acting to lower the orbital energies. The valence MO levels in F_{16}PcFe are uniformly shifted downward (by ∼1.5 eV) as compared to those in H_{16}PcFe for the same $^3A_{2g}$ state. (Since in F_{16}PcFe the ^3E_g state is nearly degenerate with $^3A_{2g}$, Figure 2 also presents the MO energy levels for the former state, and it may be seen that the two states differ in their d-orbital energies and ordering.) Upon substitution of eight peripheral F-atoms with CF_3-groups, as occurs in going from F_{16}PcFe to F_{32}PcFe, there is additional downshift of the MO levels, consistent with higher overall electronegativity of the CF_3 group. Because the ground electronic state of F_{32}PcFe is different than that of F_{16}PcFe, the magnitude of this shift varies from one d-orbital to the next. For example, the d_{z^2} and d_π orbitals are lower to a lesser extent than is d_{xy}. The transition from F_{32}PcFe to F_{48}PcFe shifts the MO levels down by about 0.2 eV, but the MO pattern is essentially unchanged.

Table 2 provides a comparison of the Fe−N(eq) bond lengths obtained by RKS and UKS calculations. $R_{Fe-N}{}^{RKS}$ values lie quite close to $R_{Fe-N}{}^{UKS}$, suggesting that spin contamination in these systems is small, and the relative energies in Table 1 can be considered reasonably reliable.

The gross populations of Fe 3d, 4s, and 4p orbitals are reported in Table 3, along with the atom's Mulliken atomic charge. The "effective" charge of Fe increases on going from H_{16}PcFe (0.74 e) to F_{48}PcFe (0.88 e), but the difference in Q_{Fe} between F_{32}PcFe and F_{48}PcFe is only 0.01 e. The Fe 3d and 4p populations are ∼6.59 and ∼0.26 e, respectively, and are insensitive to the substitution of the Pc ring. In contrast, the population of the Fe 4s orbital decreases as the level of fluorosubstitution rises; again, there is little change beyond F_{32}.

Table 4. Calculated Fe−Phthalocyanine Binding Energies (E_{bind}'s), Ionization Potentials (IPs), and Electron Affinities (EAs), All in Units of eV

		H_{16}PcFe	F_{16}PcFe	F_{32}PcFe	F_{48}PcFe
E_{bind}		9.82	9.55	9.94	10.02
IP[a]	a_{1u}	6.39 (1st)	7.84 (1st)	8.71 (1st)	8.91 (1st)
	a_{1g}/d_{z^2}	6.43	7.88	10.63	10.82
	b_{2g}/d_{xy}	6.60	8.06	9.90	10.11
	$1e_g/d_\pi$	7.24	8.69	8.92	9.10
	b_{1u}	8.01	9.13	9.85	10.05
EA[a]		−2.55 ($1e_g$)	−4.06 ($1e_g$)	−5.44 (b_{2g})	−5.69 (b_{2g})

[a] See Figure 2 for orbital energy levels.

Table 4 presents the calculated values of the Fe−phthalocyanine binding energies (E_{bind}'s), ionization potentials (IPs) (for several outer MOs), and electron affinities (EAs). E_{bind} is defined as the energy required to pull the Fe apart from the macrocycle ring. In the case of H_{16}PcFe, for example, we have

$$-E_{bind} = E(H_{16}PcFe) - \{E(Fe) + E(H_{16}Pc)\}$$

where $E(H_{16}PcFe)$, $E(Fe)$, and $E(H_{16}Pc)$ represent the total energies of H_{16}PcFe, Fe, and H_{16}Pc, respectively. (The geometries of H_{16}PcFe and H_{16}Pc are independently optimized.)

The IPs and EAs were calculated by the so-called ΔSCF method which computes each property as the difference in total energy between the neutral and ionized species.

The calculated binding energy of 9.8 eV for H_{16}PcFe is reduced slightly for F_{16}PcFe, suggesting that the peripheral F substituents weaken the interaction between the metal and the ring by some 0.27 eV. The opposite effect, a strengthened interaction, however, is connected with the presence of CF_3 or C_2F_5 substituents; the strongest binding occurs for F_{48}PcFe.

The calculations associate the a_{1u} orbital of the ring with the lowest IP for all of the systems examined, even though it lies below the metal a_{1g} and $1e_g$ orbitals. The calculated first IP of 6.39 eV for H_{16}PcFe is in excellent agreement with the photoelectron spectra (PES) value of 6.36 eV, measured for H_{16}PcFe in the gas phase.[24] Corresponding to the downshift of the valence MOs, the IPs of the substituted molecules are considerably higher than those of H_{16}PcFe. The first IPs of F_{16}PcFe, F_{32}PcFe, and F_{48}PcFe are 7.84, 8.71, and 8.91 eV, respectively. Paralleling the MO energy levels in Figure 2, there is a systematic increase of 0.2 eV in the IPs on going from F_{32}PcFe to F_{48}PcFe.

This pattern is repeated for the electron affinities indicated in the last row of Table 4. Beginning with a calculated EA of 1.5 eV for H_{16}PcFe, this quantity rises by 1.5 eV in F_{16}PcFe, and by another 1.4 eV upon going to F_{32}PcFe. The further fluorosubstitution associated with F_{48}PcFe raises the EA by only an additional 0.25 eV.

3.2. Effects of Axial Ligands. The next point to be considered involves the effects of a pair of axial ligands upon

(22) In DFT, Janak's theorem (ref 23) states that, for the ground state, only the lowest orbitals or spin-orbitals are occupied and all empty ones are higher or degenerate.

(23) Janak, J. F. *Phys. Rev. B* **1978**, *18*, 7165.

(24) Berkowitz, J. *J. Chem. Phys.* **1979**, *70*, 2819.

Table 5. Calculated Relative Energies (eV) for Different Species (D_{2h}) Containing Axial Ligands L

configuration					$E^{relative}$		
d_{xy}	d_{z^2}	d_{yz}	d_{xz}	state[a,b]	L = Ace	L = H_2O	L = Py
				$H_{16}PcFe(L)_2$			
2	2	1	1	$^3B_{1g}$ ($^3A_{2g}$)	*c*	0.60 (1.927/2.633)	1.92 (1.930/2.796)
2	1	2	1	$^3B_{2g}$ [^3E_g(A)]	0 (1.936/2.337)[d]	0 (1.936/2.264)	1.01 (1.938/2.355)
1	1	2	2	$^3B_{1g}$ ($^3B_{2g}$)	0.17 (1.928/2.382)	0.18 (1.929/2.283)	1.15 (1.932/2.352)
2	0	2	2	$^1A_{1g}$ ($^1A_{1g}$)	0.15 (1.945/1.962)	0.05 (1.941/2.002)	0 (1.940/2.013)
				$F_{16}PcFe(L)_2$			
2	2	1	1	$^3B_{1g}$ ($^3A_{2g}$)	0.58 (1.927/2.870)	0.63 (1.930/2.656)	2.15 (1.933/2.740)
2	1	2	1	$^3B_{2g}$ [^3E_g(A)]	0 (1.934/2.314)	0 (1.934/2.259)	1.11 (1.940/2.347)
1	1	2	2	$^3B_{1g}$ ($^3B_{2g}$)	0.21 (1.926/2.342)	0.20 (1.925/2.275)	1.28 (1.931/2.349)
2	0	2	2	$^1A_{1g}$ ($^1A_{1g}$)	0.11 (1.943/1.965)	0 (1.937/2.001)	0 (1.937/2.030)
				$F_{32}PcFe(L)_2$			
2	2	1	1	$^3B_{1g}$ ($^3A_{2g}$)	0.74 (1.931/2.759)	0.83 (1.934/2.580)	2.33 (1.937/2.705)
2	1	2	1	$^3B_{2g}$ [^3E_g(A)]	0 (1.937/2.291)	0.04 (1.938/2.251)	1.14 (1.940/2.347)
1	1	2	2	$^3B_{1g}$ ($^3B_{2g}$)	0.17 (1.926/2.323)	0.20 (1.927/2.275)	1.25 (1.928/2.346)
2	0	2	2	$^1A_{1g}$ ($^1A_{1g}$)	0.07 (1.943/1.970)	0 (1.941/2.001)	0 (1.930/2.034)

[a] States in parentheses refer to the corresponding designations in unligated PcFe. [b] No minimum Fe−L distance was found for the $(d_{xy})^1(d_{z^2})^2(d_{yz})^2(d_{xz})^1$ − $^3B_{3g}$ [^3E_g(B)] state. [c] No minimum Fe−L distance. [d] Values in parentheses represent the optimized Fe−N(Pc) and Fe−L bond lengths (in Å), respectively.

the electronic structure and properties of $H_{16}PcFe$, $F_{16}PcFe$, and $F_{32}PcFe$. (The previous section has shown that the smaller $F_{32}PcFe$ mimics the essential properties of the larger $F_{48}PcFe$.) The axial ligands considered here include acetone (Ace), H_2O, and pyridine (Py). Considering its π-type MOs, Py represents a relatively strong-field ligand, and it is well-known for its ability to coordinate Fe^{II} complexes. While both Ace and H_2O possess electron pairs to coordinate the central metal, neither contains appropriate π-MOs, and thus they have weaker coordinating properties. Concerning the geometry of the ligated iron phthalocyanines, each axial ligand was attached to Fe with the O or N atom pointing toward the metal; the molecular plane of the axial ligand was perpendicular to phthalocyanine, bisecting its N−Fe−N angles. This geometry has been observed in the X-ray crystal structures of $[H_{16}PcFe(4Me\text{-}Py)_2]$[25] and $F_{64}PcFe(Py)_2$.[2c]

The coordination of the two axial ligands lowers the symmetry to D_{2h} and splits the d_{xz}−d_{yz} degeneracy. Relative energies of the various $S = 1$ states were computed, along with the singlet. (A high-spin $S = 2$ state is unlikely to be a ground state for the ligated systems in view of the very high energy of the $b_{1g}/d_{x^2-y^2}$ orbital.) The results for $H_{16}PcFe(L)_2$, $F_{16}PcFe(L)_2$, and $F_{32}PcFe(L)_2$ (L = Ace, H_2O, Py) are reported in Table 5, along with the optimized Fe−N(eq) (Pc) and Fe−L bond lengths of each state. The states are listed in the same order as in Table 1, to more clearly emphasize changes in the energy ordering caused by the axial ligands. One obvious difference with the four-coordinate system is that double occupation of the d_{z^2} orbital, as in the $^3B_{1g}$ ($^3A_{2g}$ in unligated PcFe) and $^3B_{3g}$ [^3E_g(B)] states, results in infinite or a very long Fe−L distance, which implies that $^3B_{1g}$ ($^3A_{2g}$) is no longer the ground state in $H_{16}PcFe(L)_2$ and $F_{16}PcFe(L)_2$.

3.2.1. Electronic Structure. The first and perhaps most important effect of the ligands has to do with the $^3A_{2g}$ state. While this is the ground electronic state, or at least nearly so, for all the R_fPcFe systems in Table 1, the situation is clearly quite different when the ligands are added. The $^3A_{2g}$ state ($^3B_{1g}$ after the ligands are added) lies between 0.6 and 0.8 eV higher than the ground state for L = Ace or H_2O, and even higher for L = Py.

The ground state of $H_{16}PcFe(Ace)_2$ is calculated to be $^3B_{2g}$ $[(d_{xy})^2(d_{z^2})^1(d_\pi)^3]$ (which corresponds to the ^3E_g(A) state in $H_{16}PcFe$); the same is true for both $F_{16}PcFe(Ace)_2$ and $F_{32}PcFe(Ace)_2$. The closed-shell $^1A_{1g}$ is the second lowest state, 0.15 eV higher in energy. This energy gap is lowered to 0.11, and then 0.07 eV, respectively, for $F_{16}PcFe(Ace)_2$ and $F_{32}PcFe(Ace)_2$. Slightly higher in all three cases is the $^3B_{1g}$ state. The triplet $^3B_{2g}$ is also the ground state for $H_{16}PcFe(H_2O)_2$, although $^1A_{1g}$ lies very close in energy. Indeed, these two states are indistinguishably close in $F_{16}PcFe(H_2O)_2$, and then they reverse in $F_{32}PcFe(H_2O)_2$. In all three systems, the $^3B_{1g}$ state lies about 0.2 eV higher. There is no ambiguity concerning the ground state for strong-field Py ligands, where the $^1A_{1g}$ state is separated from the others by at least 1 eV. Whether $H_{16}PcFe(Py)_2$, $F_{16}PcFe(Py)_2$, or $F_{32}PcFe(Py)_2$, the next two states in order of increasing energy are $^3B_{2g}$ and then $^3B_{1g}$. Summarizing, although the electronic configuration of a ligated iron phthalocyanine is governed mainly by the axial ligand-field strength, this otherwise intrinsic property also depends on the peripheral substituents.

The calculated results appear to agree with available experimental information. The computations for $F_{16}PcFe(Ace)_2$ are consistent with early magnetic measurements[4] that indicate the complex is of intermediate spin. The prediction of a low-spin ground state for $F_{32}PcFe(Py)_2$ is in full agreement with experiment.[2c]

Figure 4 illustrates the manner in which the MO energies are affected by the nature of the ligands, comparing $H_{16}PcFe$ with $H_{16}PcFe(Ace)_2$, $H_{16}PcFe(H_2O)_2$, and $H_{16}PcFe(Py)_2$. Owing to repulsive interactions, the principal effect of the axial ligands is to raise the energy of the a_{1g} (d_{z^2}) orbital. In general, the stronger the axial ligand field, the greater the

(25) Cariati, F.; Morazzoni, F.; Zocchi, M. *J. Chem. Soc., Dalton Trans.* **1978**, 1018.

Table 6. Calculated Properties of $H_{16}PcFe$, $F_{16}PcFe$, and $F_{32}PcFe$ with Two Axial Ligands at the Ground State

	$H_{16}PcFe(L)_2$			$F_{16}PcFe(L)_2$			$F_{32}PcFe(L)_2$		
L:	Ace ($^3B_{2g}$)	H_2O ($^3B_{2g}$)	Py ($^1A_{1g}$)	Ace ($^3B_{2g}$)	H_2O ($^1A_{1g}$)	Py ($^1A_{1g}$)	Ace ($^3B_{2g}$)	H_2O ($^1A_{1g}$)	Py ($^1A_{1g}$)
$R_{Fe-N(Pc)}$ (Å)	1.936	1.936	1.940 (1.935)[a]	1.934	1.937	1.937	1.937	1.941	1.939 (1.938)[b]
R_{Fe-L} (Å)	2.337	2.264	2.013 (2.040)[a]	2.314	2.001	2.030	2.291	2.001	2.034 (2.038)[b]
E_{bind}[PcFe−(L)$_2$] (eV)	0.22	0.26	1.88	0.58	0.52	2.26	0.83	0.73	2.54
Q_{Fe} (e)	0.78	0.84	0.63	0.82	0.85	0.66	0.81	0.84	0.66
IP[c,d] (eV)	6.10 (a_{1g})	6.28 (a_{1g})	6.13 (b_{1g})	7.22 (a_{1g})	7.73 ($1b_{3g}$)	7.49 (b_{1g})	7.94 (a_{1g})	8.58 ($1b_{3g}$)	8.23 (b_{1g})
	5.72 ($1b_{3g}$)	**5.90** ($1b_{3g}$)	**5.97** ($1b_{3g}$)	**7.13** ($1b_{3g}$)	7.92 (b_{1g})	**7.33** ($1b_{3g}$)	**7.93** ($1b_{3g}$)	8.67 (b_{1g})	**8.12** ($1b_{3g}$)
	6.01 (b_{1g})	6.10 (b_{1g})	6.04 ($1b_{2g}$)	7.41 (b_{1g})	**7.56** (a_{1u})	7.41 ($1b_{2g}$)	8.15 (b_{1g})	**8.47** (a_{1u})	8.21 ($1b_{2g}$)
	5.97 (a_{1u})	6.16 (a_{1u})	5.99 (a_{1u})	7.37 (a_{1u})	7.93 ($1b_{2g}$)	7.36 (a_{1u})	8.27 (a_{1u})	8.78 ($1b_{2g}$)	8.25 (a_{1u})
EA[c] (eV)	−2.29 ($1b_{2g}$)	−2.40 ($1b_{2g}$)	−1.70 ($2b_{3g}$)	−3.72 ($1b_{2g}$)	−3.90 (a_{1g})	−3.10 ($2b_{3g}$)	−4.71 ($1b_{2g}$)	−4.89 (a_{1g})	−4.15 ($2b_{3g}$)
			−1.68 (a_{1g})		−3.19 ($2b_{3g}$)	−3.04 (a_{1g})		−4.28 ($2b_{3g}$)	−3.97 (a_{1g})

[a] The values in parentheses are experimental distances for $PcFe(4Me\text{-}Py)_2$ (ref 25). [b] The values in parentheses are experimental distances for $F_{64}PcFe$ (ref 2c). [c] See Figure 4 for the orbitals in parentheses. [d] The first IP is indicated in bold.

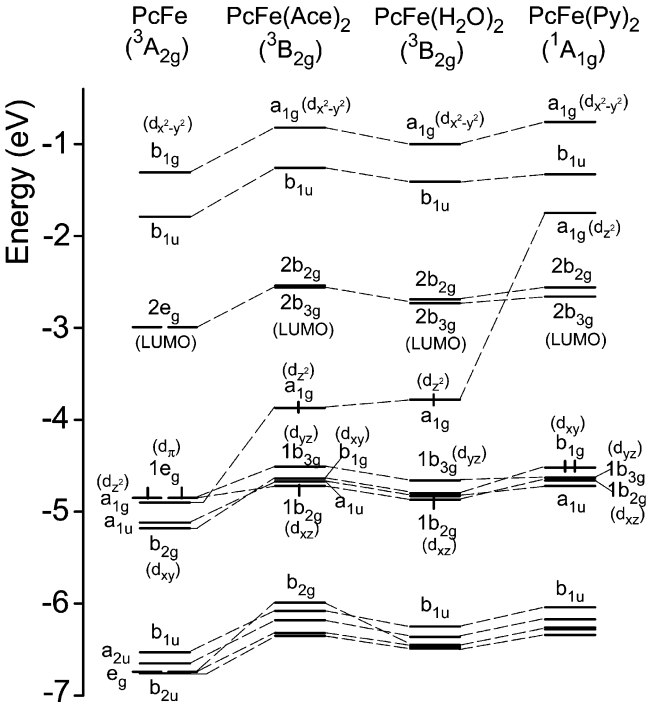

Figure 4. Orbital energy levels of $H_{16}PcFe$ when complexed with a pair of axial ligands.

d_{z^2}-orbital destabilization, and the more likely it is that a low-spin state will be observed. In $H_{16}PcFe(Py)_2$, the large elevation of the a_{1g} orbital results in a low-spin complex. In contrast, the axial coordination of Ace or H_2O leads to a smaller rise in a_{1g}, permitting it to be singly occupied. (While the MO energy level diagram shows $1b_{2g}$ below $1b_{3g}$, it is the latter that contains the other odd electron.)

3.2.2. Structural and Energetic Properties. The calculated properties of the various iron phthalocyanines with two axial ligands, in their ground states, are collected in Table 6, together with available experimental data.[2c,25] The equatorial Fe−N(eq) distance in the ligated systems shows a certain amount of core expansion (~0.02 Å) as compared to that in unligated $H_{16}PcFe$. This distance is relatively insensitive to the nature of the ligand, as well as to the degree of fluorosubstitution. Owing to occupation of the $3d_{z^2}$ orbital, the axial Fe−L distance in $H_{16}PcFe(L)_2$ for L = Ace or H_2O is considerably longer than that in $H_{16}PcFe(Py)_2$, and it is in fact close to the Co−N(axial) bond length in PcCo(4Me-Py)$_2$,[25] where an unpaired electron is localized in the $3d_{z^2}$ orbital of Co^{II}. While the Fe···Py distance is almost independent of fluorosubstitution, both the Fe···Ace and Fe···H_2O distances contract as more F atoms are added to the system. It is gratifying to note that the calculated Fe−N(eq) and Fe−N(Py) distances are in good agreement with the X-ray crystal structural data of similar systems.[2c,25]

The binding energies (E_{bind}'s) reported in Table 6 refer to the energetics of adding the two axial ligands to the system. This quantity is in the 0.2−0.3 eV range for Ace and H_2O bound to $H_{16}PcFe$ but grows to nearly 1 eV as the latter is fluorosubstituted. Py, on the other hand, is bound much more strongly. Its binding energy is 1.9 eV for $H_{16}PcFe$ and grows to as much as 2.5 eV for $F_{32}PcFe$. In contrast to $H_{16}PcFe(Ace/H_2O)_2$, where the ligands increase the positive charge on Fe, the Py ligands decrease this charge, indicating a flow of electrons to Fe.

Unlike $H_{16}PcFe$, where the first ionization occurs from a Pc orbital, that of $H_{16}PcFe(L)_2$ takes place from a metal d-orbital ($1b_{3g}/d_{yz}$). This result is in agreement with experimental observation on $H_{16}PcFe(Py)_2$.[26] Owing to upshifts of the MOs, the IPs of $H_{16}PcFe(L)_2$ are decreased notably as compared to those of $H_{16}PcFe$, suggesting that the former will be easier to oxidize than unligated $H_{16}PcFe$. The axial ligands also reduce the electron affinity, especially for L = Py. Note that the added electron in $[H_{16}PcFe(Py)_2]^-$ occupies a high-lying antibonding Pc $2b_{3g}$ orbital, whereas the added electron in $H_{16}PcFe$ goes into a low-lying bonding orbital to yield a $[H_{16}Pc^{2-}Fe^{I}]^-$ species. The calculated redox properties of $H_{16}PcFe$ are in agreement with electronic spectroscopy and electron spin resonance (ESR) measurements on the positive and negative ions.[27]

For fluorosubstituted $F_{16}PcFe(Ace)_2$ and $F_{16}PcFe(Py)_2$, the first ionization occurs from the $1b_{3g}$ (d_{yz}) orbital, similar to the case of $H_{16}PcFe(L)_2$. For $H_{16}PcFe(H_2O)_2$, however, the IP from the Pc a_{1u} orbital is lowest (if a closed-shell ground state is considered for this system), and the EA corresponds to the addition of an electron to the a_{1g} (d_{z^2}) orbital. $F_{32}PcFe(L)_2$ behaves similarly to $F_{16}PcFe(L)_2$ except that the

(26) Lever, A. B. P.; Wilshire, J. P. *Inorg. Chem.* **1978**, *17*, 1145.
(27) (a) Clack, D. W.; Yandle, J. R. *Inorg. Chem.* **1972**, *11*, 1738. (b) Myers, J. F.; Canham, G. W.; Lever, A. B. P. *Inorg. Chem.* **1975**, *14*, 461. (c) Minor, P. C.; Gouterman, M.; Lever, A. B. P. *Inorg. Chem.* **1985**, *24*, 1894.

Table 7. Comparison of Relative State Energies (eV) among Different Computational Methods on Iron Porphine (PFe)

state	VWN-B-P[a]	VWN-B-P[b]	B3LYP[c]	CPMD[d]	LDF[e]	CASPT2[f]	MRMP[g]	exptl
$^3A_{2g}$	0	0	0	0	0	0	0	0
^3E_g (A)	0.12	0.08	0.27		−0.19	0.02	−0.23	0.07[h]
$^3B_{2g}$	0.26	0.22	0.62		0.39	0.59	−0.05	
^3E_g (B)	0.74		0.92			1.05	0.40	
$^5A_{1g}$	0.71	0.67	0.30	0.64	1.33	−0.83	−0.60	0.62[i]
^5E_g	0.85	0.77	0.54			−0.69	−0.41	
$^5B_{2g}$	1.05	0.95	0.77		1.57	−0.54	−0.23	
$^1A_{1g}$	1.49	1.36	1.67		1.05	1.50	−0.06	

[a] Present ADF calculations using VWN-B-P functional and triple-ζ basis sets (see also ref 11). [b] ADF calculations by Kozlowski et al. using VWN-B-P functional and double-ζ basis sets on the C/N/H atoms (ref 10d). [c] DFT calculations by Kozlowski et al. using hybrid B3LYP functional (ref 10d). [d] DFT calculations by Rovira et al. based on the Carr−Parrinello Molecular Dynamics method (ref 10c). [e] Local density functional calculations by Matsuzawa et al. (ref 10b). [f] Multiconfigurational second-order perturbation calculations with complete active space self-consistent field (CASSCF) reference functions, by Choe et al. (ref 29). [g] Multireference Møller−Plesset perturbation calculations by Choe et al. (ref 29). [h] Reference 30. [i] Reference 31.

calculated IP and EA values for the former system are significantly larger.

4. Conclusions

The ground electronic state of $H_{16}PcFe$ is $^3A_{2g}$, with ^3E_g and $^3B_{2g}$ slightly higher (<0.1 eV) in energy. The first quintet and singlet are well separated from these triplets. Introduction of the electron-withdrawing peripheral substituents on the Pc ring progressively lowers the ^3E_g and $^3B_{2g}$ states. As a result, the three triplet states are nearly degenerate for $F_{16}PcFe$, and $^3B_{2g}$ becomes the ground state for $F_{32}PcFe$. No further changes occur when the CF_3 groups in $F_{32}PcFe$ are replaced by C_2F_5. The strong similarity of the calculated results between $F_{32}PcFe$ and $F_{48}PcFe$ suggests that either system can mimic the essential properties of the fully fluorinated $F_{64}PcFe$. That is, CF_3 groups can be safely replaced by F atoms, so long as the latter are separated from the phenyl ring by the requisite single C-atom.

The fluorosubstitution progressively lowers the energies of the individual molecular orbitals. It is the differential changes among the highest occupied MOs that account for the aforementioned changes in ground state. These orbital shifts are also responsible for the strengthened binding energies of Fe to the macrocycle, and the increased ionization potentials and electron affinities. The latter effects would lead to the prediction of more difficult oxidation and more favorable reduction for more highly fluorosubstituted species. Again, these quantities are rather similar for $F_{32}PcFe$ and $F_{48}PcFe$.

The electronic structure and properties of $H_{16}PcFe$ are influenced by axial ligand coordination. First and foremost, the $^3A_{2g}$ state, with its double d_{z^2} occupancy, is raised considerably in energy and is no longer the ground state, not even for unfluorinated $H_{16}PcFe(L)_2$. When two weak-field axial ligands (Ace or H_2O) coordinate, $H_{16}PcFe(L)_2$ exhibits a $^3B_{2g}$ intermediate-spin state. Fluorosubstitution, however, leads to a progressive stabilization of the low-spin $^1A_{1g}$ state. While this effect is insufficient to alter the nature of the ground state for L = Ace, $^1A_{1g}$ becomes the ground state for $F_{32}PcFe(H_2O)_2$. In the case of L = Py, the strong-field ligands raise the energy of the Fe $3d_{z^2}$-orbital to a larger degree, thereby making the Fe^{II} ion diamagnetic in a $^1A_{1g}$ ground state. The latter remains unambiguously the ground state for L = Py, even as the system is fluorosubstituted.

The Py ligands are bound much more strongly than are the acetone and water. While the Fe···Py distance is almost independent of fluorosubstitution, both the Fe···Ace and Fe···H_2O distances contract as more F atoms are added to the system. The axial ligands also induce a certain amount of core expansion within the PcFe systems. The ionization potential of all species is reduced by axial ligation, as is the electron affinity. In contrast to $H_{16}PcFe$, the first IP in $H_{16}PcFe(L)_2$ corresponds to removal of an electron from a metal d-orbital. Therefore, the coordination of axial ligands can change not only the redox potentials but also the redox site of the system, as observed experimentally.[28] It should be pointed out that when adding or removing an electron from a metal 3d-orbital, the Mulliken population analysis does not yield a charge difference of unity between Q_{Fe} in $[PcFe]^{1+/-}$ and Q_{Fe} in $[PcFe]^0$. In fact, the atomic charge on the metal is changed by only a little, as the Pc macrocycle plays the role of an electron buffer in the metal oxidation and reduction.[8] This behavior is understandable because the charge tends to delocalize over the entire conjugated molecule in order to reduce the electron−electron repulsion. Nevertheless, experiments are able to determine whether the oxidation/reduction takes place at the metal or at the macrocycle ring, and the calculated redox sites can be compared to experimental results.

Taken together, these calculations suggest ways to obtain new phthalocyanine materials and catalysts whose steric and electronic properties could be designed in a rational fashion taking into account the effects of the ligand and metal substituents.

Acknowledgment. This work was supported by Grant DAAD19-99-1-0206 (to S.S.) from the Army Research Office, and, in part, by Air Products and Chemicals (to S.M.G.).

Appendix 1. ADF Calculations on Iron Porphine (PFe)

There have been a number of prior theoretical calculations on iron porphine (PFe) with various computational methods, providing a data set by which to assess the present ADF formalism. The calculated relative energies for different states

(28) (a) Kadish, K. M.; Li, J.; Van Caemelbecke, E.; Ou, Z. P.; Guo, N.; Autret, M.; D'souza, F.; Tagliatesta, P. *Inorg. Chem.* **1997**, *36*, 6292. (b) Cocolios, P.; Kadish, K. M. *Isr. J. Chem.* **1985**, *25*, 138.

Table 8. Calculated Relative Energies (E's, eV) for Different Configurations of $H_{16}PcFe$, $F_{16}PcFe$, and $F_{32}PcFe$, with VWN-PW91x-PW91c and X_α Functionals

configuration[a]					$E(R)$[b]		
b_{2g}/d_{xy}	a_{1g}/d_{z^2}	$1e_g/d_\pi$	$b_{1g}/d_{x^2-y^2}$	state	$H_{16}PcFe$	$F_{16}PcFe$	$F_{32}PcFe$
					With VWN-PW91x-PW91c Functional[c]		
2	2	2	0	$^3A_{2g}$	0 (1.913)[b]	0 (1.915)	0 (1.917)
2	1	3	0	^3E_g (A)	0.04 (1.921)	0.00 (1.921)	−0.05 (1.923)
1	1	4	0	$^3B_{2g}$	0.07 (1.918)	0.03 (1.918)	−0.08 (1.917)
1	2	3	0	^3E_g (B)	0.52 (1.907)	0.52 (1.908)	0.44 (1.909)
1	2	2	1	$^5A_{1g}$	1.17 (1.975)	1.14 (1.969)	1.15 (1.969)
1	1	3	1	^5E_g	1.20 (1.981)	1.11 (1.975)	1.08 (1.973)
2	1	2	1	$^5B_{2g}$	1.54 (1.979)	1.46 (1.968)	1.45 (1.974)
2	0	4	0	$^1A_{1g}$	1.38 (1.935)	1.32 (1.933)	1.24 (1.933)
					With X_α Functional[d]		
2	2	2	0	$^3A_{2g}$	0 (1.887)	0 (1.889)	0 (1.892)
2	1	3	0	^3E_g (A)	−0.13 (1.894)	−0.15 (1.896)	−0.21 (1.898)
1	1	4	0	$^3B_{2g}$	0.00 (1.893)	−0.04 (1.893)	−0.17 (1.892)
1	2	3	0	^3E_g (B)	0.34 (1.882)	0.33 (1.883)	0.25 (1.883)
1	2	2	1	$^5A_{1g}$	0.98 (1.952)	0.96 (1.944)	0.95 (1.950)
1	1	3	1	^5E_g	0.88 (1.957)	0.82 (1.951)	0.74 (1.955)
2	1	2	1	$^5B_{2g}$	1.29 (1.956)	1.23 (1.944)	1.19 (1.956)
2	0	4	0	$^1A_{1g}$	1.64 (1.906)	1.60 (1.909)	1.50 (1.909)

[a] Orbital energy levels illustrated in Figure 2. [b] Values in parentheses refer to optimized Fe−N(eq) bond length (in Å) for the pertinent state. [c] Local spin-density functional of Vosko, Wilk, and Nusair (VWN)[14] plus Perdew−Wang's 1991 gradient correction for exchange (PW91x)[34] and Perdew−Wang's 1991 gradient correction for correlation (PW91c).[34] [d] Simple X_α functional ($\alpha = 0.7$).

in PFe are presented in Table 7, together with the results obtained by other DFT[10b−d] and advanced ab initio methods[29] from the recent literature. Available experimental data[30,31] are listed in the last column of the table for comparison.

One essential question concerns the ground state configuration of the Fe^{II} ion. It is generally accepted that the ground state is intermediate spin ($S = 1$), and only the $^3A_{2g}$ state is compatible with Mössbauer, magnetic, and proton NMR data.[30,31] From a theoretical perspective, early Hartree−Fock (HF) calculations[32] on PFe agree with experiment that $^3A_{2g}$ is indeed the most stable of various triplet states but find a high-spin $^5A_{1g}$ state to be even lower in energy by more than 1 eV. The inclusion of correlation[32] helps to repair this artificial advantage of the quintet but does not fully reverse the incorrect order of spin multiplicities. In the same vein, recent high-quality CASPT2 and MRMP studies[29] of PFe by Choe et al.[29] remain in disagreement with experiment in predicting the lowest state to be $^5A_{1g}$. The large magnetic moment observed for the iron porphyrin ($\mu_{eff} = 4.4\ \mu_B$) was thought by these authors to support their high-spin ground state. However, detailed ligand-field calculations[31] concluded that this large moment is based upon a coupling between the $^3A_{2g}$ and ^3E_g states. Moreover, the core size of the porphyrin ring of the $^5A_{1g}$ state is considerably larger than the experimental finding. When coupled with the correlation between Fe−N bond length and spin state,[33] this core size of the iron porphyrin is incompatible with a high-spin ground state but rather argues for an intermediate-spin sate.

Probably the best and most accurate calculations on the electronic structure of PFe to date are the recent ADF calculations by Kozlowski et al.,[10d] who found the ground state to be $^3A_{2g}$, in agreement with most of the experiments. The calculated relative energies compare particularly favorably with the available experimental data. Our results calculated with the same ADF program and density functional show slight differences from those of Kozlowski et al., because we have employed higher-quality basis sets on the nonmetal C/N/H atoms as compared to the calculations by Kozlowski et al.

Appendix 2. Effects of Different Density Functionals upon Calculated Relative Energies

To examine possible effects of different density functionals on the calculated relative energies, a comparison with two other functionals, VWN-PW91x-PW91c and X_α, was carried out on the three unligated $H_{16}PcFe$, $F_{16}PcFe$, and $F_{32}PcFe$ molecules. PW91x and PW91c refer, respectively, to Perdew−Wang's 1991 gradient correction to exchange and Perdew−Wang's 1991 gradient correction to correlation;[34] X_α represents the simple X_α functional with $\alpha = 0.7$. The results are displayed in Table 8.

Compared to Table 1, the VWN-PW91x-PW91c and VWN-B-P functionals yield similar results for both R_{Fe-N} and $E^{relative}$, the differences being less than 0.01 Å and 0.05 eV, respectively. Importantly, the order of the relative energies calculated with VWN-B-P is the same as that obtained with VWN-PW91x-PW91c. The experimental Fe−N bond length in solid $H_{16}PcFe$ is about 1.93 Å,[35] very close to the VWN-PW91x-PW91c or VWN-B-P calculated value of 1.92 Å for the ground state.

For X_α, however, the predicted Fe−N bond lengths of the various states are notably shorter than those obtained by the VWN-PW91x-PW91c functional. As a result, the underes-

(29) Choe, Y.-K.; Nakajima, T.; Hirao, K.; Lindh, R. *J. Chem. Phys.* **1999**, *111*, 3837.
(30) Lang, G.; Spartalian, K.; Reed, C. A.; Collman, J. P. *J. Chem. Phys.* **1978**, *69*, 5424.
(31) Boyd, P. D. W.; Buckingham, A. D.; McMecking, R. F.; Mitra, S. *Inorg. Chem.* **1979**, *18*, 3585.
(32) For a review of early HF and CI calculations on PFe, see ref 10d.
(33) Scheidt, W. R.; Reed, C. R. *Chem. Rev.* **1981**, *81*, 543.
(34) Perdew, J. P.; Chevary, J. A.; Vosko, S. H.; Jackson, K. A.; Pederson, M. R.; Singh, D. J.; Fiolhais, C. *Phys. Rev. B* **1992**, *46*, 6671.
(35) Kirner, J. F.; Dow, W.; Scheidt, W. R. *Inorg. Chem.* **1976**, *15*, 1685.

timation of the bond lengths yields a significant lowering of the relative energy for $^3E_g(A)$, and this state is clearly the ground state for $H_{16}PcFe$, in disagreement with experiment. Both $F_{16}PcFe$ and $F_{32}PcFe$ have a $^3E_g(A)$ ground state too at the X_α level. These results indicate that the nonlocal gradient corrections (to the local density functional) play an important role in the calculations of the relative energies. But even at the X_α level, an obvious trend is that the relative energy of $^3B_{2g}$ decreases on going from $H_{16}PcFe$ to $F_{32}PcFe$, consistent with the VWN-PW91x-PW91c or VWN-B-P results.

Supporting Information Available: Bibliographic information on structurally characterized hexacoordinated Fe(II) phthalocyanines with $R < 7\%$. This material is available free of charge via the Internet at http://pubs.acs.org.

IC035263J